BNL-113326-2016-JA

Potassium and Water Coadsorption on TiO2(110): OH-Induced Anchoring of Potassium and the Generation of Single-Site Catalysts

David C. Grinter, Elena Rodríguez Remesal, Si Luo, Jaime Evans, Sanjaya D. Senanayake, Dario J. Stacchiola, Jesus Graciani, Javier Fernández Sanz, and José A. Rodriguez

Submitted to Journal of Physical Chemistry Letters

October 2016

Chemistry Department

Brookhaven National Laboratory

U.S. Department of Energy
USDOE Office of Science (SC),
Basic Energy Sciences (BES) (SC-22)

DISCLAIMER

Potassium and Water Co-Adsorption on TiO_2(110): OH-induced Anchoring of Potassium and the Generation of Single-site Catalysts

David C. Grinter,[a] Elena Rodríguez Remesal,[b] Si Luo,[a,c] Jaime Evans,[d] Sanjaya D. Senanayake,[a] Dario J. Stacchiola,[a] Jesus Graciani,[b] Javier Fernández Sanz[b,*] and José A. Rodriguez [a,c*]

[a] *Chemistry Department, Brookhaven National Laboratory, Upton, NY, 11973, United States*

[b] *Departamento de Química Física. Universidad de Sevilla. 41012-Sevilla. SPAIN*

[c] *Department of Chemistry, State University of New York (SUNY) at Stony Brook, Stony Brook, New York, 11794, United States*

[d] *Facultad de Ciencias, Universidad Central de Venezuela, Caracas 1020 A, Venezuela*

Abstract

Potassium deposition on TiO_2(110) results in reduction of the substrate and the formation of loosely bound potassium species which can move easily on the oxide surface to promote catalytic activity. The results of density functional calculations predict a large adsorption energy (~ 3.2 eV) with a small barrier (~ 0.25 eV) for diffusion on the oxide surface. In scanning tunneling microscopy images, the adsorbed alkali atoms lose their mobility when in contact with surface OH groups. Furthermore, K adatoms facilitate the dissociation of water on the titania surface. The K-(OH) species generated are good sites for the binding of gold clusters on the TiO_2(110) surface producing Au/K/TiO_2(110) systems with a high activity for the water-gas shift.

TOC Graphic

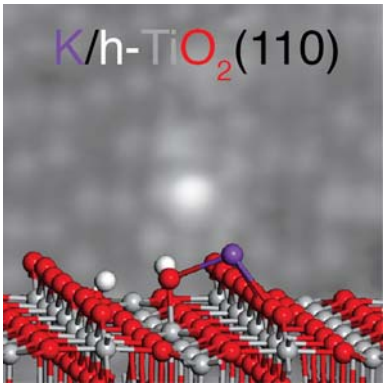

Alkali metals act as promoters of heterogeneous catalysts in a very wide range of important chemical processes (ammonia synthesis, CO oxidation, NO reduction, alcohol synthesis from CO/CO_2 hydrogenation, the water-gas shift reaction, Fischer-Tropsch synthesis, olefin epoxidation, etc.).[1] The precise mechanisms behind the alkali promotional effects are not yet fully understood.[2] In principle, an alkali can participate directly in a catalytic process or it can modify the chemical properties of the catalyst components.[3] Most catalysts used in the chemical industry combine metals and oxides. The study of the co-adsorption of alkali metals and simple molecules on well-defined surfaces of transition metals has been a favored topic of research for almost a century since the pioneering work by Langmuir in 1923.[4] To explain the effects of alkalis on the surface chemistry of metals, the following mechanisms have been proposed in the literature: (1) site-blocking effects, (2) through-the-metal electronic interactions, (3) through-the-space electronic interactions (e.g., electrostatic), (4) direct chemical interactions, and (5) alkali-induced surface reconstructions.[4-7] In comparison, much less is known about the interaction of alkali metals with well-defined surfaces of oxides.[8-17] Recently, it has been shown that the addition of sodium or potassium to water-gas shift (WGS, $H_2O + CO \rightarrow H_2 + CO_2$) catalysts which contain gold or platinum produces a substantial increase in catalytic activity by inducing the formation of single-site (Pt or Au)-$O(OH)_x$-(Na or K) species.[18-20] Active sites that contain only a metal center are formed as a consequence of interactions of the metal with $(OH)_x$-(Na or K) groups. It is not clear how these groups are formed by the reaction of the alkali with water molecules.

In this work, we investigate the behaviour of ultralow coverages of potassium in the $K/TiO_2(110)$ and $\{K+H_2O\}/TiO_2(110)$ systems using a combination of scanning tunneling microscopy (STM), photoemission, and calculations based on density-functional theory (DFT). K atoms display a very high mobility on the titania substrate. The adsorption energy of the alkali is large but there is a low barrier for diffusion. This could facilitate a close contact between the alkali and adsorbates essential for catalytic promotion. Furthermore, the potassium adatoms facilitate the dissociation of water, forming (OH)-K units that have a very low mobility on the $TiO_2(110)$ substrate. When water is pre-dosed on titania, the species acts as a nucleation site for potassium atoms and the formed (OH_t)-K units are proposed to be excellent sites for the binding of metals such as Au or Pt.

An oxidized o-$TiO_2(110)$ surface is characterized by a low density of point defects, and the appearance in empty-states STM (Figure 1a) is dominated by bright rows running along the [001] direction, corresponding to Ti_{5c}, with a few oxygen adatoms located on top of these rows (triangular highlight).[12]

Upon exposure to a very low coverage of potassium (1.35% ML) at 300 K, the surface displayed in Figure 1b is formed; it has a significant number of hydroxyl species in bridging (OH_b) and terminal (OH_t) positions (hexagonal highlight in Figure 1b, total coverage 2% ML) which are identified in STM by their locations between and on top of the Ti_{5c} rows and their ability to be removed by voltage pulses from the STM tip. A number of tall (250-300 pm) species are also observed (highlighted with a circle) which interact heavily with the tip as evidenced by streaking in the images, we assign these as highly mobile potassium clusters. Their binding to the surface is so weak that after a single scan over a region of the surface they are no longer visible, even under relatively gentle tunnelling conditions. Further exposure to the same amount of potassium (total 2.7% ML) approximately double the hydroxyl concentration (5% ML) due to dissociation of water present in the background gases of the chamber (Figure 1c). The concentration of large K species is also increased (circular highlight), these were observed to be slightly more stable under the STM tip than at the lower coverage (it took a couple of STM scans under normal conditions to clear the area of adsorbates), this suggests some stabilization in the presence of additional OH_b. The ratio between the concentration of OH and the calibrated K dose is of the order of 2:1, this is consistent with the formation of two hydroxyl groups per K atom deposited via reaction with background H_2O within the chamber (p ~1×10^{-9} Torr).[21] It is important to note that due to the facile movement of K by the STM tip, the K coverage observed in imaging is much lower than the calibrated dose. (0.24% ML vs. 2.7% ML).

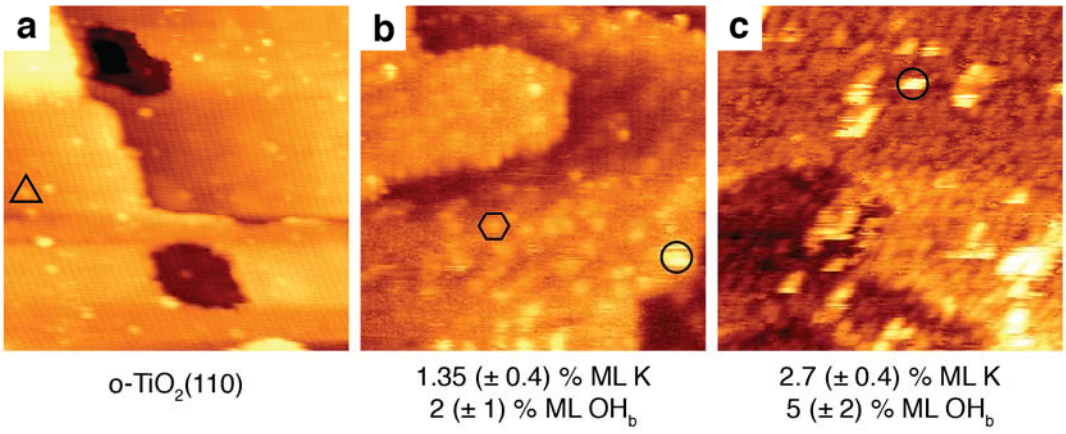

Figure 1. Sequential evaporation of K onto o-TiO_2(110) at 300 K. (30 × 30 nm^2, V = +1.74 V, I = 0.11 nA)

XPS spectra of o-TiO_2(110) upon adsorption of potassium are displayed in S.I. Figure S1. As observed in the STM images in Figure 1, there is reduction of the TiO_2 surface upon K adsorption (Figure S1a),

concomitant with an increase in OH_b species and partially oxidized K, consistent with previous studies of K/TiO_2.[22-24]

Water is prevalent in many real catalytic situations in which alkali metals are present and has important effects in the reactivity of TiO_2(110). The results of K/o-TiO_2(110) in Figure 1 suggested that OH groups played a role in stabilizing the potassium species. To probe this further, we prepared a fully hydroxylated h-TiO_2(110) surface, where all the oxygen vacancies are reacted with water to form a high concentration of OH_b species[12], prior to depositing potassium at 300 K, the results of which are displayed in Figure 2. One additional motivation for pre-hydroxylating these surfaces is from a practical point of view – the as-prepared TiO_2(110) surfaces are very reactive to any background water in the UHV system and within a few hours a mixture of vacancies and hydroxyl species can be observed. In order to have a more controlled system consisting of only hydroxyls, we therefore chose to expose to water prior to potassium evaporation.

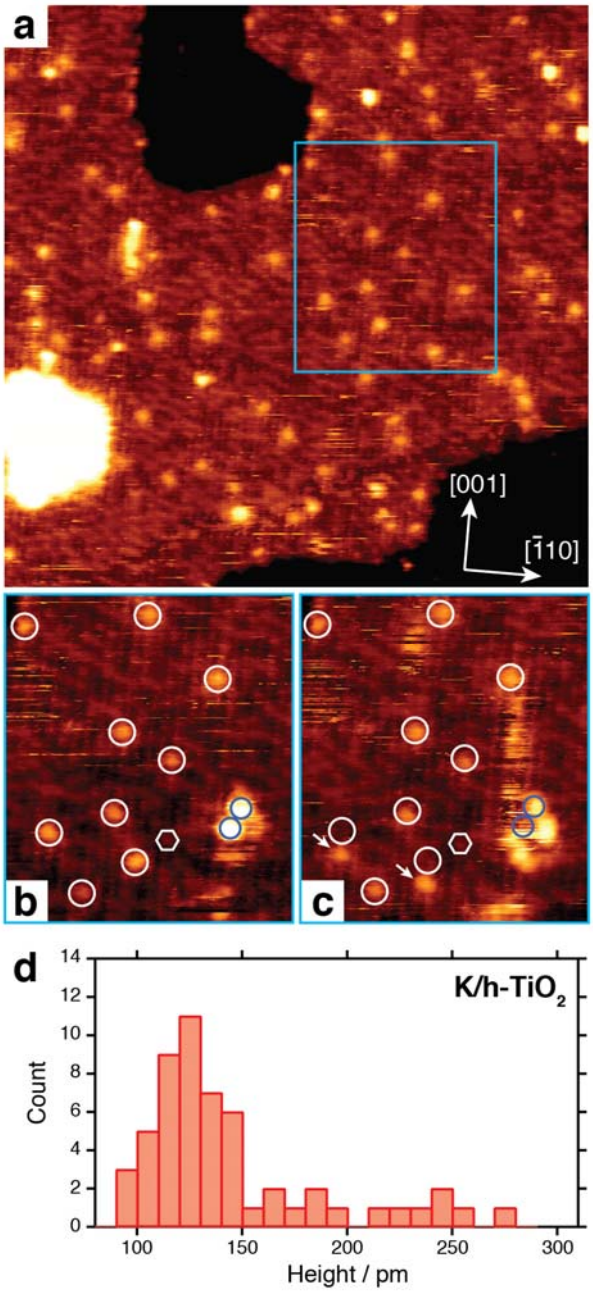

Figure 2. The structure and mobility of 0.6% ML K on h-TiO_2(110). **(a)** 50 × 50 nm^2 image acquired immediately after evaporation of K, **(b)** & **(c)** 17 × 20 nm^2 images of the blue highlighted section in (a) acquired sequentially afterwards, demonstrating the tip-induced movement of K species. (V = +1.78 V, I = 0.10 nA) **(d)** height distribution of the K species.

In the large area image in Figure 2a we see a uniform distribution of atomic-sized bright features across the surface, with no nucleation at step edges, implying a relatively strong interaction with the h-TiO_2(110). Interestingly this is an opposite effect to that observed for atoms of less reactive metals such as Au, where the presence of OH_b facilitates their diffusion across the surface, leading to nucleation at

the step edges.[25] These bright features are assigned as K species and their concentration is consistent with the dose. (0.6% ML) The stability of the potassium is markedly higher than on the o-TiO_2(110) with the majority of the atoms remaining nearly immobile over many tens of scans (hours) under similar tunnelling conditions. Figure 2b & 2c show expanded views of the region highlighted in Figure 2a and were obtained from sequential STM scans. The potassium atoms are highlighted with circles, and an OH_b with a hexagon. Two of the atoms (white arrows) move upwards a short distance along the [001] direction. Despite the [001] being the slow scan direction for these images, the anisotropy of the TiO_2(110) surface results in a much lower barrier for diffusion along [001] compared to [1-10].[26] In addition to the movement of these two atoms, the much taller feature marked by purple circles also shows a clear shift, with a bright streak becoming visible in Figure 3c. The enhanced mobility of potassium species along [001] was also observed in an earlier work by Yurtsever et al. using NC-AFM,[13] although in that case the attractive interaction with the AFM tip is likely to be stronger than for the STM. The OH_b concentration is measured to be 18(±1) % ML, a slight increase from before dosing K (16(±2) % ML), and importantly is significantly more than observed for K/o-TiO_2(110). (5(±2) % ML) This correlates well with the increased stability for the potassium under STM scanning when comparing K/h-TiO_2(110) to K/o-TiO_2(110). A histogram of the height distribution for the potassium species obtained from STM imaging is displayed in Figure 2d. It is roughly trimodal with the majority of the K having a height of ~120 pm, which can be attributed to single atomic species. Taller features with heights in the ranges 150-200 pm and 220-270 pm are also observed, originating either from K species containing multiple atoms, or possibly KOH/KO_x. For comparison, the heights of OH_b under these imaging conditions is 50 (±10) pm, this is quite variable as it is dependent on the termination of the STM tip as well as the tunnelling current and bias voltage.[27] The XPS spectra for potassium deposited on the hydroxylated surface also show reduction of the TiO_2 and the generation of additional OH_b species, along with the formation of partially oxidized K. (S.I. Figure S2)

To precisely identify the binding sites of the potassium species, high resolution STM images were acquired, an example of which is displayed in Figure 3a. The round yellow features (hexagonal highlight) are OH_b (see Figure 3b), these permit accurate positioning of the bridging O rows (white lines in Figure 3a). The potassium species have a green/blue colour and can be broadly separated into

two types according to their height: type *i*, highlighted with squares, are 100-150 pm tall and type *ii*, highlighted with circles, are 200-250 pm tall. The binding sites are between the bridging O rows, with the taller species located in the three-fold hollow sites between the in-plane and bridging oxygen atoms, as shown in the structural model in Figure 3b, consistent with NC-AFM studies of this system.[11,13] The model surface depicted in Figure 3b highlights the different hydroxyl species that are commonly observed on the TiO_2(110) surface, namely bridging hydroxyls (OH_b) which comprise hydrogen atoms on top of the bridging oxygen rows (O_{br}), and terminal hydroxyls (OH_t) which are located on top of the Ti_{5c} sites.

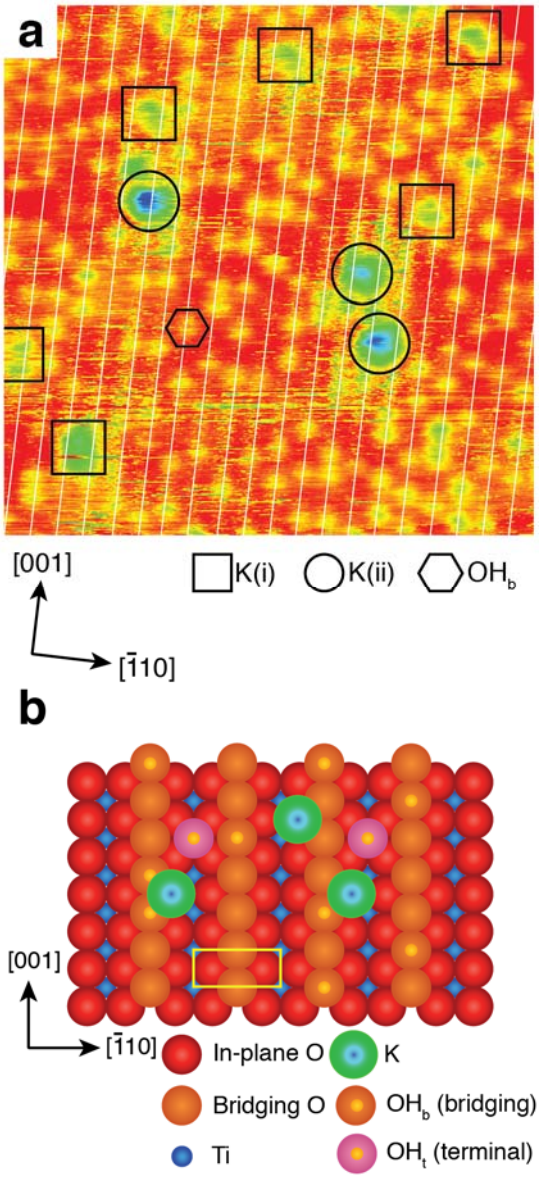

Figure 3. Binding sites of 0.6% ML K on h-TiO_2(110). **(a)** STM image (13 × 13 nm^2, V = +1.78 V, I = 0.10 nA) and **(b)** ball model demonstrating the binding locations of the K species. The positions of the bridging O rows along [001] are indicated in the STM image by white lines.

From the experimental measurements described above one can conclude that K has a large mobility on the titania surface. DFT calculations were used to study the bonding and mobility of K deposited on the o-TiO_2(110) surface. First of all, deposition of potassium gives rise to K^+ ions and reduction of the substrate with formation of Ti^{3+} species located in the subsurface layer, consistent with the XPS observations. (see S.I. for details) The potential energy surface (PES) for the adsorption was systematically scanned on a quarter of a (1x1) cell and the data for the relative energies, referred to the minimum, is plotted in Figure 4a. The most stable adsorption configuration corresponds to a K^+ ion bonded to two oxygen atoms in an O bridging row of o-TiO_2(110) as depicted in Figure 4b. The adsorption energy is 3.24 eV indicating a strong interaction. The K-O distance is 2.57 Å and the height of K above the titania surface (O bridging plane) is 2.11 Å.

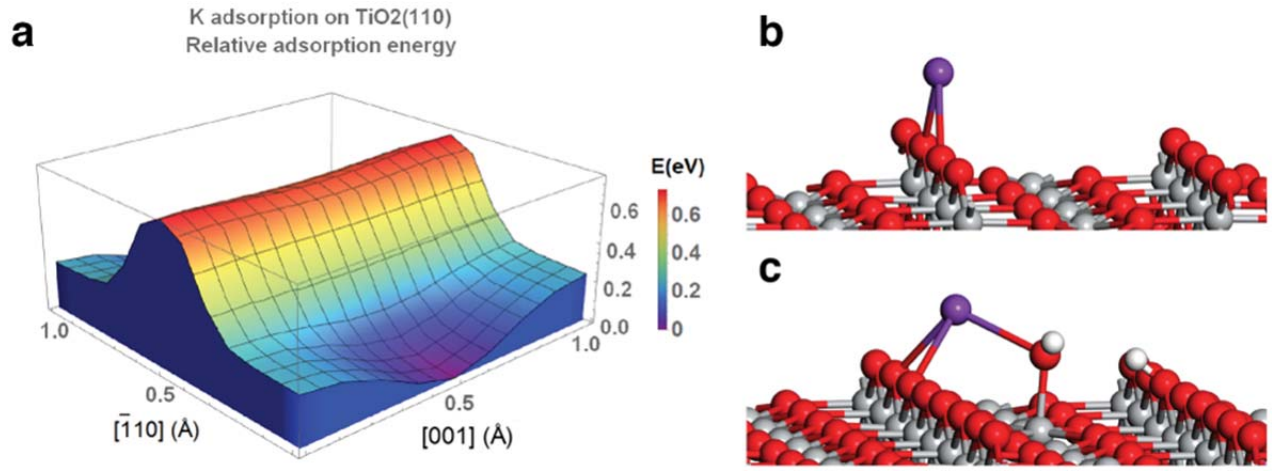

Figure 4. (a) DFT potential energy surface for the diffusion of a K atom over a (1x1) cell of the TiO_2(110) surface. The reference for energy is the minimum that corresponds to configuration in Figure 4b and the coordinate origin for the [001] and [$\bar{1}$10] directions is set to the position of a bridging oxygen atom, fractional coordinates (0,0). **(b)** Structure of the most stable adsorption site for K/o-TiO_2(110). **(c)** Optimized structure of a K-OH species adsorbed on the h-TiO_2(110) surface.

The calculations indicate that there is a low barrier for the movement of K along the atoms in the O bridging rows, Figure 4a. The potassium moves along the [001] direction from a minimum, where it

bridges two O atoms, to a local maximum on top of a single O_{br} atom, and there moves forward (backwards) to another minimum. The estimated energy barrier is 0.24 eV and can be easily overcome at room temperature or at the high temperatures used for most catalytic processes. Thus, one is dealing with an adsorbate that has the peculiarity of having a strong binding energy and a high mobility on the surface. This is ideal for promotional effects[3] since the alkali can get closer to other adsorbates on the surface of the oxide.

The scenario completely changes when water molecules are co-adsorbed together with K atoms because the presence of the alkaline atoms favors the water dissociation stabilizing surface hydroxyl groups. Water adsorption and dissociation on the TiO_2(110) surface has been examined in several papers and the dissociation process has been reported to be endothermic by 0.13-0.18 eV.[28-30] In Table 1, the energies obtained from DFT+*U* optimizations and reference single point calculations carried out using a hybrid exchange-correlation functional are reported. The results indicate that, whatever the model is, the adsorption energy is ~1 eV, while the dissociation is exothermic by 0.14-0.21 eV. The release of energy upon dissociation significantly increases to -0.39 eV when K atoms are present. The geometry of the minimum energy structure for water dissociated on the K/TiO_2(110) surface is reported in Figure 4c where formation of a K-OH_t species is clearly seen. This matches well with the observed structure in STM in Figure 3a where the position of the K species (assumed to be a K-OHt complex on the basis of the DFT) is between the bridging oxygen and Ti_{5c} rows. Furthermore, in experiments of XPS we observed a larger sticking coefficient and rate of the dissociation for water on K/TiO_2(110) than on plain TiO_2(110), in agreement with the theoretical calculations. Experiments for the low temperature (< 200 K) deposition of potassium on water films supported on titania led to the formation of $K_n(OH)_m$ aggregates.

	E_{ads}(mol)	E_{ads}(dis)	ΔE
TiO_2 (110) 6 layers	-1.02	-1.17	-0.15
TiO_2 (110) 4 layers	-1.05	-1.22	-0.17
TiO_2 (110) 4 layers HSE06	-0.94	-1.15	-0.21
K/TiO_2 (110) 6 layers	-1.00	-1.39	-0.39

Table 1. Adsorption energies (eV) for water on the TiO_2(110) surface from DFT+*U* and HSE06 calculations. E_{ads}(mol): molecularly adsorbed; E_{ads}(dis): dissociated water; $\Delta E = E_{ads}(dis) - E_{ads}(mol)$.

In summary, our DFT calculations show that deposited K atoms can easily move on the surface jumping between minima connected through small barriers (0.24 eV). In fact, the interaction energy between potassium and a couple of bridging oxygen atoms next to a neighboring OH_t group is 3.20 eV, i.e. almost that obtained for the perfect titania surface. Eventually a K^+ ion finds an OH_t group where is it trapped, forming a highly stable K-OH_t species, Figure 4c. The whole process might be visualized as either a stronger interaction between K atoms and TiO_2(110) surface mediated by OH_t groups (E_{ads} for K increase by 0.26 eV) or a more favored water dissociation fostered by the presence of K atoms on the surface (ΔE lowers from -0.15 to -0.39 eV, Table 1) which results in the formation of one terminal hydroxyl (OH_t) and one bridging hydroxyl (OH_b).

From previous studies it is known that K adatoms affect the growth and size distribution of gold nanoparticles on TiO_2(110).[9,10] In order to identify the effect of hydroxylated potassium on the adsorption of small metal nanoparticles, we evaporated a small amount of Au onto the K/h-TiO_2(110) surface at 300 K after mapping the positions of the K species. The results of this are shown in Figure 5, with Figure 5a the potassium-dosed surface, and Figure 5b the complete system; potassium and Au clusters are highlighted with green and yellow circles, respectively. The Au clusters have a height ranging from 0.4 to 0.9 nm (2-3 atomic layers), and a total density of 0.01 nm^{-2} (corresponds to a total gold coverage of ~0.1 ML). From this data we observe that although many of the Au clusters nucleate at the step edges, due to their high mobility on the hydroxylated surface, consistent with the work of Matthey et al.[25], a number are sited directly above potassium species on the TiO_2(110) terraces – these are marked with white asterisks in Figure 5b. After acquiring a number of such in-situ evaporation images for the Au/K/TiO_2(110) system, we observe that approximately 33(±4)% of the Au clusters on the TiO_2(110) terraces are located directly above a potassium site, although this is not a majority it does indicate the potential for important interactions between the gold and the potassium. Other studies have found that the K-(OH) groups seen in Figures 3 and 4 can attract gold or platinum atoms to form single-site Au-K(OH) species that can catalyze the water-gas shift reaction[18-20] and the conversion of CO_2 into alcohols.[31] Indeed, in kinetic tests of catalytic activity, we found that a Au/K/TiO_2(110) surface was a much better catalyst for the water-gas shift than Au/TiO_2(110), Figure 5c. In the presence of the alkali, the rate for the production of hydrogen increases 3-4.5 times and the apparent activation energy drops from 10 to 7 kcal/mol. The very high catalytic activity observed for the Au-K-(OH) species during the water-gas shift reaction (refs [18-20] and Figure 5c) may be the result of cooperative effects where the K helps with the dissociation of water and the Au with the adsorption of CO and

subsequent steps for the reaction. In this aspect, the participation of K in the reaction is crucial because Au alone cannot dissociate water.[32]

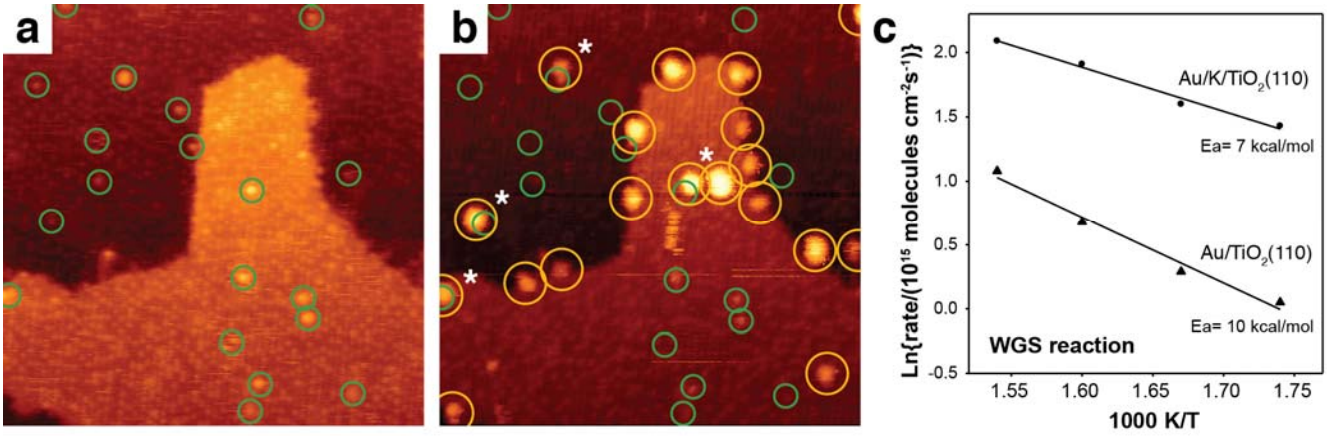

Figure 5. STM images of h-TiO_2(110) functionalized with **(a)** 0.006 ML potassium, and **(b)** 0.006 ML potassium and 0.1 ML Au. The positions of K atoms and Au clusters are highlighted with green and yellow circles, respectively. Au clusters bound in close proximity to potassium are marked with asterisks. (40 × 40 nm^2, V = +1.78 V, I = 0.10 nA). **(c)** Arrhenius plots for the production of hydrogen during the water-gas-shift on Au/TiO_2(110) and Au/K/TiO_2(110). The Au coverage in both cases is close to 0.15 ML. The potassium coverage in Au/K/TiO_2(110) is ~ 0.05 ML. P_{CO}= 20 Torr ; P_{H2O}: 10 Torr.

In conclusion, our STM and DFT studies of the interaction of K with TiO_2(110) surfaces demonstrate the pivotal role that OH groups play in this system. For the oxidized TiO_2(110) surface, the adsorption of potassium results in reduction of the surface along with the generation of highly mobile K^+ ions. This reduced surface is able to dissociate water easily, leading to the formation of OH_t species which pin the potassium on the surface as K-OH_t. Deposition on the hydroxylated TiO_2(110) surface also results in formation of stable K-OH_t species. The evaporation of small gold clusters onto this surface indicates that the potassium can provide sites for nucleation of the gold, which may prove to be relevant when considering alkali metal promotion effects for Au/TiO_2 catalysts. The strong interaction of the alkali with the oxide modifies the intrinsic vigorous reaction of K with water,[40] but the system still remains very reactive towards O-H bond cleavage.

Experimental Methods

The STM experiments were carried out in an ultrahigh vacuum (UHV) system with a base pressure of ~5×10^{-10} Torr containing an Omicron variable temperature scanning tunnelling microscope (VT-STM).

The single crystal TiO_2(110) substrates were prepared by repeated cycles of Ar sputtering and annealing in UHV to ~1000 K. The crystals had a moderate degree of bulk reduction, as typified by their dark blue colour. Potassium was deposited from a getter source whose evaporation rate was calibrated in STM. (S.I. Figure S3) Oxidised (o-TiO_2(110)) surfaces were formed by exposing the as-prepared crystal to ~10 L O_2 at 300 K. Hydroxylated (h-TiO_2(110)) surfaces were formed by exposing the as-prepared crystal to 2 L H_2O (ultrapure, 18.2 MΩ.cm, freeze-pump-thaw purified) at 300 K. The absence of oxygen vacancies on the hydroxylated surface was confirmed by performing +3 V scans with the STM tip, to selectively desorb H from the surface, as demonstrated in the supporting information. (S.I. Figure S4) The coverage of potassium is given in ML, where one monolayer is defined as one adsorbate per primitive unit cell of the TiO_2(110) surface, a density of 5.2×10^{14} cm^{-2}. XPS measurements were performed in a separate UHV chamber; the spectra were recorded using Mg Kα soft x-rays. (hν = 1253.6 eV). The kinetic tests of catalytic activity for the K/Au/TiO_2(110) and Au/TiO_2(110) systems were performed in an instrument which combines an ultra-high vacuum chamber with a high-pressure reactor following the methodology described in previous studies (P_{CO}= 20 Torr, P_{H2O}= 10 Torr, T= 550-625 K).

Theoretical Methods

DFT calculations were performed using the plane-wave-pseudopotential approach within the projector augmented wave method (PAW)[33,34] together with the GGA exchange correlation functional proposed by Perdew *et al*.[35] (PW91) as implemented in the VASP code.[36,37] A plane-wave cutoff energy of 400 eV was used. We treated the Ti (3s, 3p, 3d, 4s), K (3s, 3p, 4s) and O (2s, 2p) electrons as valence states, while the remaining electrons were kept frozen as core states. To obtain faster convergence, thermal smearing of one-electron states (k_BT = 0.05 eV) was allowed using the Gaussian smearing method to define the partial occupancies. The energy was estimated at the gamma point. In order to represent adequately the electronic structure of reduced titania, a Hubbard-like *U* term was added to Ti 3d levels using the rotationally invariant approach proposed by Dudarev *et al*.,[38] in which the Coulomb *U* and exchange *J* parameters are combined into a single parameter $U_{eff} = U - J$. The U_{eff} value for Ti 3d states was of 4.5 eV.[39]

The surface was represented by (4x2) supercell model, 18 atomic layer thick (or six TiO_2-trilayers), which is repeated into the three directions allowing a vacuum of 15 Å between the slabs. For building

the supercell model we used the optimized lattice parameters for the bulk a = 4.669Å, c = 3.025 Å. In structural optimizations the two lowest TiO_2 trilayers were kept frozen while the rest of the atoms were allowed to fully relax their atomic positions. Reference single point calculations using the HSE06 hybrid exchange-correlation functional were performed with slabs 12 atomic layer thick.

Acknowledgements

The experimental studies at Brookhaven National Laboratory were supported by the US Department of Energy, Chemical Sciences Division (DE-SC0012704). The work performed at the University of Seville was funded by the Spanish Ministerio de Economía y Competitividad, grant CTQ2015-64669-P, Junta de Andalucía, grant P12-FQM-1595, and European FEDER. Computational resources were provided by the Barcelona Supercomputing Center/Centro Nacional de Supercomputación (Spain).

Supporting Information

- XPS spectra for K/o-TiO_2(110)
- XPS spectra for K/h-TiO_2(110)
- Calibration of K deposition via STM
- Identification of OH_b species via STM

References

(1) Koel, B.E.; Kim, J. Handbook of Heterogeneous Catalysis **2008**, 1–32.

(2) Kiskinova, M.P. Poisoning and Promotion in Catalysis Based on Surface Science Concepts and Experiments. Studies in Surface Science and Catalysis, Vol. 70, Elsevier: New York, **1992**.

(3) Uner, D.O. A Sensible Mechanism of Alkali Promotion in Fischer-Tropsch Synthesis: Adsorbate Mobilities. *Ind. Eng. Chem. Res.* **1998**, *37*, 2239-2245.

(4) Bonzel, H.P. Alkali-Metal-Affected Adsorption of Molecules on Metal Surfaces. *Surf. Sci. Rep.* **1988**, *8*, 43-125.

(5) Uner, D. O.; Pruski, M.; Gerstein, B. C.; King, T. S. Hydrogen Chemisorption on Alkali Promoted Supported Ruthenium Catalysts. *J. Catal.* **1994**, *146*, 530-539.

(6) Pacchioni, G.; Bagus, P.S. Promotion by Alkali Metals: a Theoretical Analysis of the Vibrational Shift of CO Co-adsorbed with K on Cu(100). *Chemical Physics* **1993**, *177*, 373-385.

(7) Huo, C.-F.; Wu, B.-S.; Gao, P.; Yang, Y.; Li, Y.-W.; Jiao, H. The Mechanism of Potassium Promoter: Enhancing the Stability of Active Surfaces. *Angew. Chem. Int. Ed.* **2011**, *50*, 7403 – 7406.

(8) Preda, G; Pacchioni, G.; Chiesa, M.; Giamello, E. The Reactivity of CO_2 with K Atoms Adsorbed on MgO Powders. *Phys. Chem. Chem. Phys.* **2009**, *11*, 8156-8164.

(9) Kiss, A.M.; Švec, M.; Berkó, The Effect of Pre-adsorbed K on the Size Distribution of Au Nanoparticles on a TiO_2(110) Surface. *Surf. Sci.* **2006**, *600*, 3352–3360.

(10) Mutombo, P.; Kiss, A.M.; Berko, A.; Chab, V. The Effect of Potassium on the Adsorption of Gold on the TiO_2(110)-1×1 Surface. *Nanotech.* **2006**, *17*, 4112–4116.

(11) Pang, C.L.; Muryn, C.A.; Woodhead, A.P.; Raza, H.; Haycock, S.A.; Dhanak, V.R.; Thornton, G. Low-coverage Condensation of K on TiO_2(110)-1×1. *Surf. Sci.* **2005**, *583*, L147–L152.

(12) Pang, C.L.; Lindsay, R.; Thornton, G. Structure of Clean and Adsorbate-Covered Single-Crystal Rutile TiO_2 Surfaces. *Chem. Rev.* **2013**, *113*, 3887-3948.

(13) Yurtsever, A.; Sugimoto, Y.; Abe, M.; Matsunaga, K.; Tanaka, I.; Morita, S. Alkali-metal Adsorption and Manipulation on a Hydroxylated TiO_2(110) Surface Using Atomic Force Microscopy. *Phys. Rev. B* **2011**, *84*, 085413.

(14) San Miguel, M.A.; Calzado, C.J.; Sanz, J.F. Modeling Alkali Atoms Deposition on TiO_2(110) Surface. *J. Phys. Chem. B* **2001**, *105*, 1794–1798.

(15) Calzado, C.J.; San Miguel, M.A.; Sanz, J.F. Theoretical Analysis of K Adsorption on TiO_2(110) Rutile Surface. *J. Phys. Chem. B* **1999**, *103*, 480-486.

(16) Fernandez, S.; Markovits, A.; Minot, C. Coadsorption of Gold with Hydrogen or Potassium on TiO_2(110) Surface. *J. Phys. Chem. C* **2008**, *112*, 14010-14014.

(17) An, W.; Xu, F.; Stacchiola, D.; Liu, P. Potassium-Induced Effect on the Structure and Chemical Activity of the Cu_xO/Cu(111) ($x \leq 2$) Surface: A Combined Scanning Tunneling Microscopy and Density Functional Theory Study. *ChemCatChem* **2015**, *7*, 3865-3872.

(18) Yang, M.; Li, S.; Wang, Y.; Herron, J.A.; Xu, Y.; Allard, L.F.; Lee, S.; Huang, J.; Mavrikakis, M.; Flytzani-Stephanopoulos, M. Catalytically Active Au-O(OH)x- Species Stabilized by Alkali Ions on Zeolites and Mesoporous Oxides. *Science*, **2014**, *346*, 1498-1501.

(19) Yang, M.; Liu, J.; Lee, S.; Zugic, B.; Huang, J.; Allard, L.F.; Flytzani-Stephanopoulos, M. A Common Single-Site Pt(II)–O(OH)x– Species Stabilized by Sodium on "Active" and "Inert" Supports Catalyzes the Water-Gas Shift Reaction. *J. Am. Chem. Soc.* **2015**, *137*, 3470-3473.

(20) Zugic, B.; Zhang, S.; Bells, D.C.; Tao, F.; Flytzani-Stephanopoulos, M. Probing the Low-Temperature Water–Gas Shift Activity of Alkali-Promoted Platinum Catalysts Stabilized on Carbon Supports. *J. Am. Chem. Soc.* **2014**, *136*, 3238-3245.

(21) Bikondoa, O.; Pang, C.L.; Ithnin, R.; Muryn, C.A.; Onishi, H.; G. Thornton, G. Direct Visualization of Defect-Mediated Dissociation of Water on TiO_2(110). *Nature Materials* **2006**, *5*, 189–192.

(22) Casonava, R.; Prabhakaran, K.; Thornton, G. Potassium Adsorption on TiO_2(100). *J. Phys.: Condens. Matter* **1991**, *3*, S91-S95.

(23) Heise, R.; Courths, R. A Photoemission Investigation of the Adsorption of Potassium on Perfect and Defective TiO_2(110) Surfaces. *Surf. Sci.* **1995**, *331*, 1460-1466.

(24) Muscat, J.; Harrison, N.M.; Thornton, G. First-Principles Study of Potassium Adsorption on TiO_2 Surfaces. *Phys. Rev. B* **1999**, *59*, 15457-15463.

(25) Matthey, D.; Wang, J.G.; Wendt, S.; Matthiesen, J.; Schaub, R.; Laegsgaard, E.; Hammer, B.; Besenbacher, F. Enhancing Bonding of Au Nanoparticles on Oxidized TiO_2(110). *Science* **2007**, *315*, 1692–1696.

(26) Diebold, U. The Surface Science of Titanium Dioxide. *Surf. Sci. Rep.* **2003**, *48*, 53–229.

(27) Sanchez-Sanchez, C.; Gonzalez, C.; Jelinek, P.; Mendez, J.; de Andres, P.L.; Martin-Gago, J.A.; Lopez, M.F. Understanding Atomic-Resolved STM Images on TiO_2(110)-(1×1) Surface by DFT Calculations. *Nanotech.* **2010**, *21*, 405702.

(28) Shi, H. Liu, Y.-C.; Zhao, Z.-J.; Miao, M.; Wu, T.; Wang, Q. Reactivity of the Defective Rutile TiO_2(110) Surfaces with Two Binding-Oxygen Vacancies: Water Molecule as a Probe. *J. Phys. Chem. C* **2014**, *118*, 20257-20263.

(29) Oviedo, J.; Sanchez-de-Armas, R.; San Miguel, M.A.; Sanz, J.F. Methanol and Water Dissociation on TiO_2(110): The Role of Surface Oxygen. *J. Phys. Chem. C* **2008**, *112*, 17737.

(30) Wendt, S.; Matthiesen, J.; Shaub, R.; Vestergaard, E.K.; Laegsgaard, E.; Besenbacher, F.; Hammer, B. Formation and Splitting of Paired Hydroxyl Groups on Reduced TiO_2(110). *Phys. Rev. Lett.* **2006**, *96*, 066107.

(31) Ahlers, S.J.; Pohl, M.-M.; Holena, M.; Linke, D.; Kondatrenko, E.V. Direct Propanol Synthesis from CO_2, C_2H_4 and H_2 over Cs-Au/TiO_2 Rutile: Effect of Promoter Loading, Temperature and Feed Composition. *Catal. Sci. Technol.* **2016**, *6*, 2171-2180.

(32) Liu, P.; Rodriguez, J.A. Water-gas Shift Reaction on Metal Nanoparticles and Surfaces, *J. Chem. Phys.* **2007**, *126*, 164705.

(33) Kresse G.; Joubert, D. From Ultrasoft Pseudopotentials to the Projector Augmented-wave Method Phys. Rev. B **1999**, *59*, 1758.

(34) Blöchl, P.E. Projector augmented-wave method *Phys. Rev. B* **1994**, *50*, 17953.

(35) Perdew, J.; Chevary, J.; Vosko, S.; Jackson, K.; Pederson, M.; Singh, D.; Fiolhais, C. Atoms, Molecules, Solids, and Surfaces: Applications of the Generalized Gradient Approximation for Exchange and Correlation. *Phys. Rev. B* **1992**, *46*, 6671.

(36) Kresse G.; Hafner, J. Ab-initio Molecular Dynamics for Liquid Metals. *Phys. Rev. B* **1993**, *47*, 558.

(37) Kresse G.; Furthmuller, J. Efficiency of Ab-initio Total Energy Calculations for Metals and Semiconductors using a Plane-wave Basis Set. *Comput. Mater. Sci.* **1996**, *6,* 15-50.

(38) Dudarev, S. L.; Botton, G. A.; Savrasov, S. Y.; Humphreys, C. J.; Sutton, A. P. Electron-Energy-loss Spectra and the Structural Stability of Nickel Oxide: An LSDA+U Study. *Phys. Rev. B* **1998**, *57*, 1505.

(39) Plata, J. J.; Graciani, J.; Evans, J.; Rodriguez, J.A.; J. F. Sanz. Cu Deposited on CeOx-Modified TiO_2(110): Synergistic Effects at the Metal–Oxide Interface and the Mechanism of the WGS Reaction. *ACS Catal.* **2016**, *6*, 4608–4615.

(40) Mason, P.E.; Buttersack, T.; Bauerecker, S.; Jungwirth, P. A Non-Exploding Alkali Metal Drop on Water: From Blue Solvated Electrons to Bursting Molten Hydroxide. *Angew. Chemie. Int. Ed.* **2016**, *55*, 1-5.

Supporting Information

Potassium and Water Co-Adsorption on TiO_2(110): OH-induced Anchoring of Potassium and the Generation of Single-site Catalysts

David C. Grinter,[a] Elena Rodríguez Remesal,[b] Si Luo,[a,c] Jaime Evans,[d] Sanjaya D. Senanayake,[a] Dario J. Stacchiola,[a] Jesus Graciani,[b] Javier Fernández Sanz[b,*] and José A. Rodriguez [a,c*]

[a] *Chemistry Department, Brookhaven National Laboratory, Upton, NY, 11973, United States*

[b] *Departamento de Química Física. Universidad de Sevilla. 41012-Sevilla. SPAIN*

[c] *Department of Chemistry, State University of New York (SUNY) at Stony Brook, Stony Brook, New York, 11794, United States*

[d] *Facultad de Ciencias, Universidad Central de Venezuela, Caracas 1020 A, Venezuela*

Contents

XPS spectra for K/o-TiO_2(110)

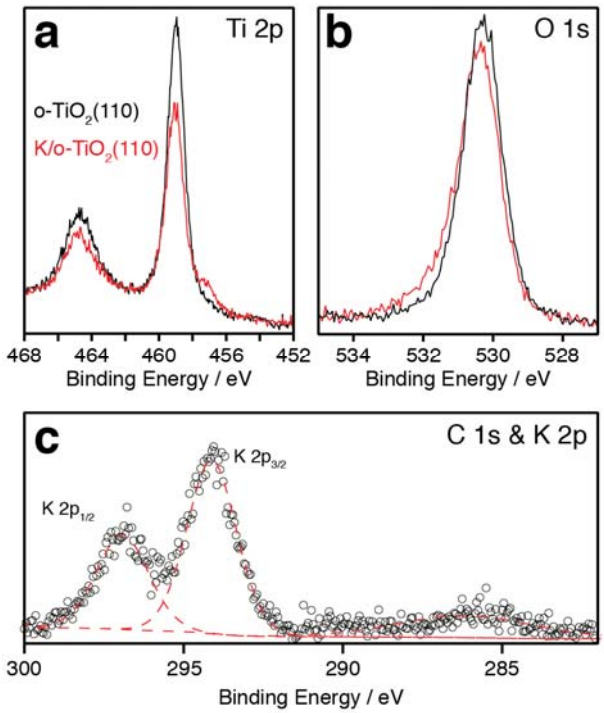

Figure S1. XPS spectra of clean (black line) and 0.3 ML potassium deposited (red line) o-TiO_2(110) at 300 K. **(a)** Ti 2p, **(b)** O 1s, **(c)** C 1s and K 2p. (hν = 1253.6 eV)

XPS spectra of o-TiO_2(110) before (black) and after (red) adsorption of potassium are displayed in Figure S1. As observed in the STM images in Figure 1, there is significant reduction of the TiO_2 surface (% Ti^{3+} goes from 5.1 to 16.7) upon K adsorption (Figure S1a), concomitant with an increase in OH_b species in the O 1s region (Figure S1b; % OH_b goes from 6.6 to 20.2), consistent with previous studies of K/TiO_2.[1-3] The corresponding K 2p and C 1s spectrum is shown in Figure S1c, the binding energy of the K $2p_{3/2}$ peak is found to be 294.2 eV, similar to that observed for K/Cr_2O_3(0001)[4] and K/MgO(001)[5], and slightly lower than the 294.4 eV reported for metallic K, suggesting a partial oxidation of the potassium.[6] The presence of metallic potassium would usually be confirmed by significant asymmetry of the 2p region with large plasmon features at higher binding energies, which are not observed in our spectra.[4,6]

XPS spectra for K/h-TiO_2(110)

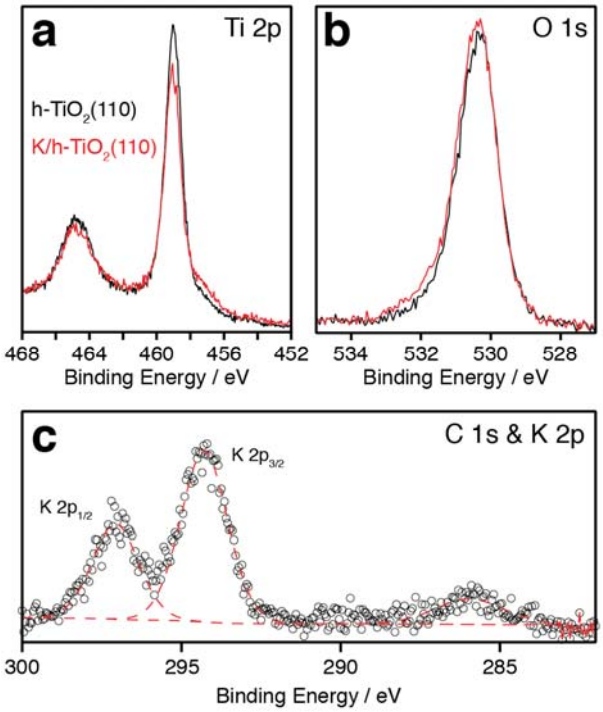

Figure S2. XPS spectra of clean (black line) and 0.3 ML potassium deposited (red line) h-TiO_2(110) at 300 K. **(a)** Ti 2p, **(b)** O 1s, **(c)** C 1s and K 2p. (hν = 1253.6 eV)

The XPS spectra for potassium deposited on the hydroxylated surface show a similar reduction of the TiO_2. (Figure S2) The Ti^{3+} component (Figure S2a) increases from 9.6 % to 23 %, as the OH_b component (Figure S2b) increases from 10.4 % to 17.2 %. The binding energy of the K $2p_{3/2}$ is 294.3 eV, consistent with that observed for K/o-TiO_2(110), for partially oxidised potassium. (Figure S2c)

Calibration of K deposition via STM

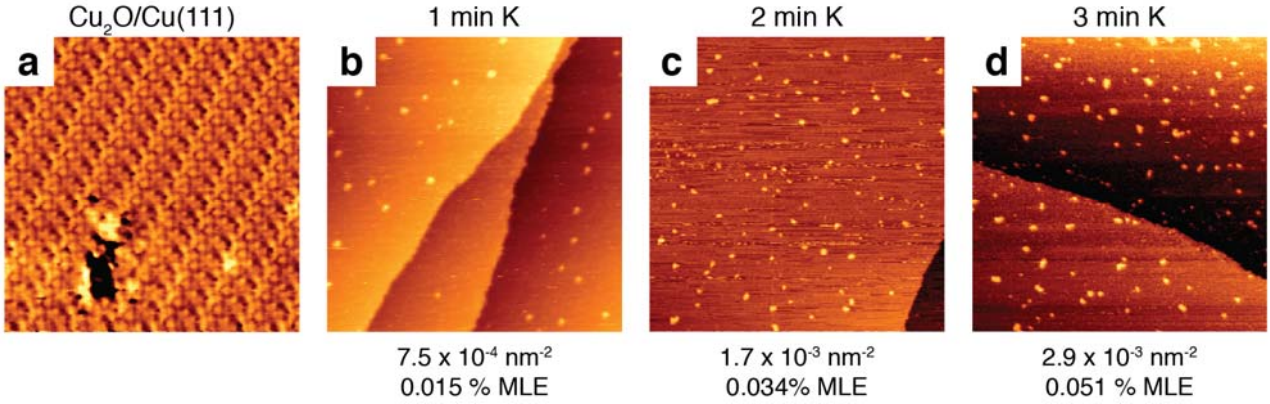

Figure S3. Calibration of K evaporation rate on $Cu_2O/Cu(111)$. (13 × 13 nm^2, V = +1.78 V, I = 0.10 nA)

Figure S3 details the calibration of the potassium evaporation rate on $Cu_2O/Cu(111)$ using STM. The clean surface is displayed in Figure S1a, with images obtained after sequential 1 minute doses shown in Figure S3b-d. The potassium nucleates as individual atomic-sized species with no mobility (either thermally or tip-induced) observed on the timescale of the STM measurement, the density and corresponding coverage in MLE are displayed under each image.

Identification of OH_b species via STM

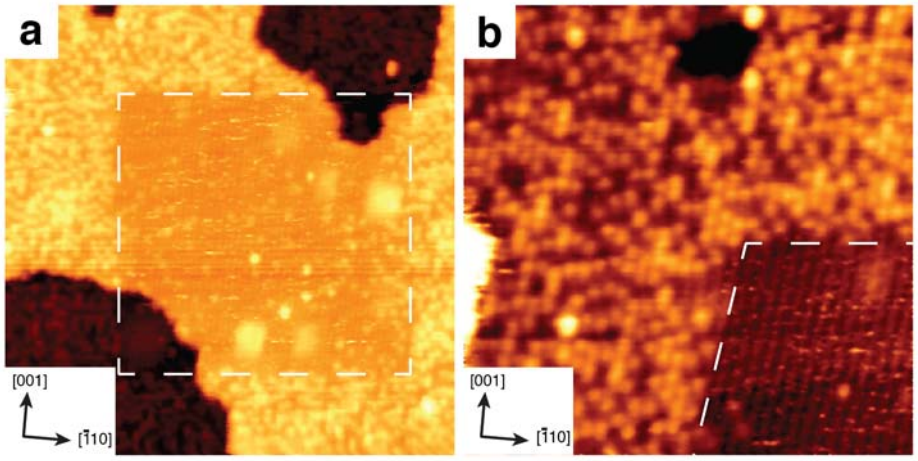

Figure S4. Removal of OH_b by 3V scans of the STM tip. The areas bordered with the dashed white lines in each image designate the high-bias scan regions. **(a)** 50 × 50 nm^2, **(b)** 22 × 22 nm^2. (V = +1.50 V, I = 0.10 nA)

High (>3 V) bias scans with the STM tip have been demonstrated to selectively desorb OH_b, yielding the pristine surface and leaving O_{vac} unaffected.[7] In Figure S4a we demonstrate the effect of performing a +3 V scan over a 30 × 30 nm^2 region of the surface marked by the dashed white line. The OH_b have been removed: in the enlarged image shown in figure S4b the bright Ti_{5c} rows can be clearly seen, along with the high density of OH_b outside of the cleared area. Using this method, we were able to check for the presence of unreacted O_{vac}, and if necessary dose with H_2O to react them in order to form the fully hydroxylated h-TiO_2(110) surfaces prior to K deposition.

References

(1) Hardman, P. J.; Casanova, R.; Prabhakaran, K.; Muryn, C. A. Electronic Structure Effects of Potassium Adsorption on TiO_2(100). *Surf. Sci.* **1992**, *269*, 677-681.

(2) Heise, R.; Courths, R. A Photoemission Investigation of the Adsorption of Potassium on Perfect and Defective TiO_2(110) Surfaces. *Surf. Sci.* **1995**, *331*, 1460-1466.

(3) Muscat, J.; Harrison, N. M.; Thornton, G. First-Principles Study of Potassium Adsorption on TiO_2 Surfaces. *Phys. Rev. B* **1999**, *59*, 15457-15463.

(4) Wilde, M.; Beauport, I.; Stuhl, F.; Al-Shamery, K.; Freund, H. J. Adsorption of Potassium on Cr_2O_3(0001) at Ionic and Metallic Coverages and UV-Laser-Induced Desorption. *Phys. Rev. B* **1999**, *59*, 13401-13412.

(5) Huang, H. H.; Jiang, X.; Siew, H. L.; Chin, W. S.; Xu, G. Q. Water Dissociation and KOH Formation on Potassium-Covered MgO/Ru(001). *Langmuir* **1998**, *14*, 7217–7221.

(6) Moulder, J. F.; Stickle, W. F.; Sobol, P. E.; Bomben, K. D. *Handbook of X-Ray Photoelectron Spectroscopy*, **2011**, 1–260.

(7) Bikondoa, O.; Pang, C. L.; Ithnin, R.; Muryn, C. A.; Onishi, H.; Thornton, G. Direct Visualization of Defect-Mediated Dissociation of Water on TiO_2(110). *Nature Mat.* **2006**, *5*, 189–192.